01338402-ComplexityProject

by Suhasan Kanagasabapathy

Submission date: 17-Feb-2020 11:01AM (UTC+0000)
Submission ID: 120159073
File name: 01338402-ComplexityProject.pdf (639.41K)
Word count: 3852
Character count: 16712

Complexity Project: The Oslo Model

Suhasan Kanagasabapathy CID: 01338402

February 17, 2020

Abstract: The self-organisation and criticality of the Oslo Model were studied. The model was implemented on Python. I focused on two main quantities of the Oslo model, which are the height of the pile and the avalanche-size probability. In each quantity, the finite-size scaling effects were studied. It was found that they follow a power law behaviour with the corresponding critical exponents, which signifies their scale-free behaviour. Using these exponents, the data could be collapsed into functions of one variable for various system sizes. For avalanche size probability, the critical exponents obtained were $\tau_s = 1.5574 \pm 0.0052$ and $D = 2.2417 \pm 0.0042$. It is remarkable to see how this scale-free behaviour emerges by just defining very simple local dynamical rules.

Word count: 2400 words in report (excluding front page, figure captions, table captions, and bibliography).

1 Task 1: Implementation of Oslo Model

The algorithm of the Oslo model described in the notes was implemented in Python. The model was built within a class object, named *Oslo*. The class contained the attributes such as the height of the pile, and the methods required for the analysis. The class was initialised with the input of the probability p for the threshold slope, the system size L, and the seed number to ensure a different realisation each time the model is run.

To test the model, the probability p was chosen as 1 since this is the BTW model where the threshold slope is always 1. A plot of the height of the pile as a function of grains added t was produced for system size $L = 16$ and shown in figure 1. There is a gradual increase in the height as well as there is no randomness. The height became a constant of 16 after the system has reached steady state. The final slope and height of the system were [1, 1, 1, ...] and [16, 15, 14, ...] respectively. This is as expected from the BTW model. For completeness, the model was tested with $p = 0$ and it returned similar result but with twice the values for the final height and slopes as expected since the allowed slope values were 2.

Next, the probability was changed to 0.5 to implement Olso model and kept it that way for the remaining of the investigation. The plot of height of the pile against t for $L = 16$ is shown in figure 2. Even though the height increases gradually, it fluctuates around a value after the steady state has been reached due to the random nature in selecting the threshold slopes. The height of the pile was averaged over time once the system has reached the steady state. For $L = 16$ and $L = 32$, the mean heights were 26.5215 and 53.9216 respectively. The measured values were close to the values mentioned in the notes [1]. Additionally as my own test, the number of distinct recurrent states, N_R for $L = 2$ and $L = 4$ were counted and compared with the analytical results from [2]. For $L = 2$, N_R obtained was 5 and for $L = 4$, N_R was 34. These values match the analytical result exactly, therefore it verifies the implementation.

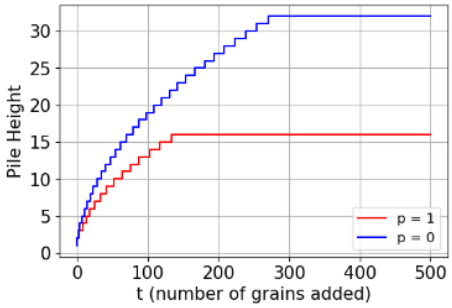

Figure 1: The pile height distribution for $L = 16$ with the probability p being 0 and 1.

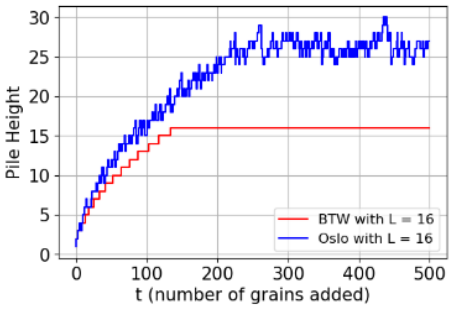

Figure 2: The pile height distribution for $L = 16$ in BTW and Oslo model with $seed = 1$. The height at steady state for Olso model is higher than in BTW model since 2 is also an allowed value for threshold slope in Oslo model.

2 Task 2: The height of the pile $h(t; L)$

The simulations for system size $L = 4, 8, 16, 32, 64, 128, 256, 512$ were completed. Different seed numbers were used to initialise the system for 5 different realisations so the height can be averaged to smooth out the data. The number of grains added is 1000000. The height of the pile is defined as

$$h(t; L) = \sum_{i=1}^{L} z_i(t) \tag{1}$$

obtained from [1].

2.1 Task 2a

Starting from an empty system, the total height of the pile was measured for the ranges of L given. The plot of height $h(t; L)$ vs. time t is given in figure 3. For all L, the height increases gradually which represents the transient stable state of the system since that particular state is never visited again. The system for all L follow the same curve for the transient configurations suggesting it could be a universal behaviour. The heights then fluctuate around constant values, which represent the stable recurrent states. From the log-log plot, it can be seen that the straight line with a positive gradient in the transient state corresponds to a power law, i.e. $h(t; L) \propto t^{\beta}$ where β is the exponent in the power law. By fitting the heights in the transient state for $L = 512$ with a power law, the exponent β obtained was 0.50670 ± 0.00002 with a constant of proportionality of 1.7125 ± 0.0004.

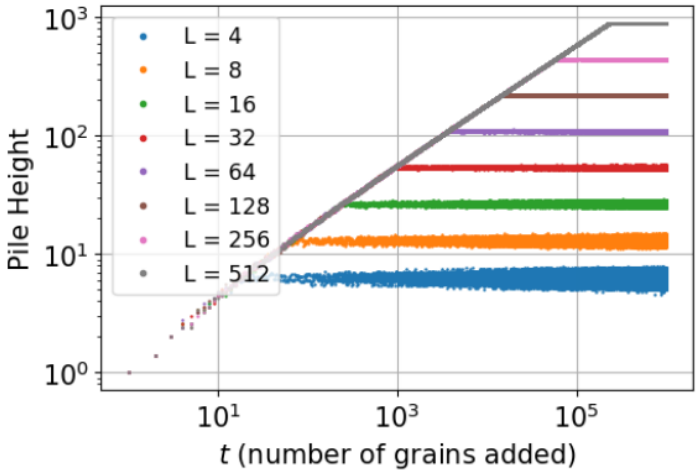

Figure 3: The log-log plot of pile height distribution for various values of L. The straight line with a positive gradient in the transient state corresponds to a power law with an exponent of 0.50670 ± 0.00002.

2.2 Task 2b

The cross-over time, t_c is the number of grains in the system before an added grain induces another grain to leave the system for the first time, i.e. $t_c = \sum_{i=1}^{L} z_i \cdot i$, obtained from [1]. The cross-over time was measured and averaged over the 5 different realisations. A plot of the average of cross-over time, $\langle t_c \rangle$ against the various system sizes L was plotted as shown in figure 4. The straight line with a positive gradient in the log-log plot clearly shows $\langle t_c \rangle$ obeys a power law. The last four points were fitted with a power law since they represent $L \gg 1$ to a good degree. The exponent obtained was 2.015 ± 0.001 with the constant of proportionality of 0.783 ± 0.007. The agreement to the power law suggests $\langle t_c \rangle$ has a universal behaviour for system sizes $L \gg 1$.

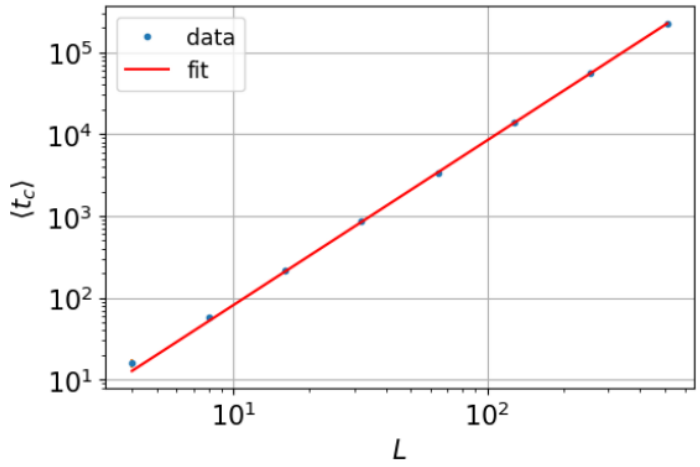

Figure 4: The log-log plot of average cross-over time $\langle t_c \rangle$ as a function of system size L. The red line represents $\langle t_c \rangle = 0.783 L^{2.015}$. $\langle t_c \rangle$ for small L deviate slightly from the fit line. The errors were obtained the standard deviation of the samples, yet there were too small to be visible in the log-log plot.

2.3 Task 2c

In this section, the scaling behaviour of average of height $\langle h \rangle$ in the steady state with the system sizes $L \gg 1$ was studied theoretically. Let us first consider the case of probability $p = 1$ (BTW model). Using eq. (1), $\langle h \rangle$ is simply L since z_i is always 1. Meanwhile in the case of $p = 0$, $\langle h \rangle$ is $2L$ since z_i is always 2. Since $\langle h \rangle$ scales linearly in both cases, it should be the same behaviour in the case of Oslo model where the probability is 0.5. Similarly, using the definition of cross-over time in task 2b, the average cross-over time $\langle t_c \rangle$ in the case of probability p being 1 and 0, are $L(L+1)/2$ and $L(L+1)$ respectively. Both values scale as L^2 for $L \gg 1$. Hence, $\langle t_c \rangle$ in the Oslo model should also scale as L^2 for large L. This agrees well with the numerical result for the exponent obtained in task 2b, which is close to 2 for large L.

2.4 Task 2d

The height $\tilde{h}$ was processed as described in task 2a to smooth out the data. From the previous task, we know that $\tilde{h} \propto L$ and $\langle t_c \rangle \propto L^2$. It was suspected $\tilde{h}$ should scale linearly with L for $L \gg 1$ and this is characterised by a scaling function F such that $\tilde{h} = LF(x)$ where x is t/L^2. To perform the data collapse, the dependence on L in the expression of $\tilde{h}$ was removed. Hence, I plotted $\tilde{h}/L$ as a function of t/L^2 and the plot is shown in figure 5(a). There is a sharp cutoff around $t/L^2 = 1$ for separating the transient and the steady state. Here, the scaling function $F(x)$ behaves like a power law for $x \ll 1$ indicating in the transient state, the height increases according to a power law, as observed in task 2a. For large arguments $x \gg 1$, the scaling function behaves as a constant to indicate the system has reached steady state. From the expression for $\tilde{h}$ obtained above, I could predict that in the transient state, $\tilde{h} \propto \sqrt{t}$ since $\tilde{h} \propto L$ and $t \propto L^2$. This is indeed what was obtained in task 2a, giving the exponent of t as 0.50654 in the transient state. However, the exponent was not very close to 0.5 and this could be due to the condition of $L \gg 1$ to get $t \propto L^2$. The larger the L, the closer we could get to the desired exponent.

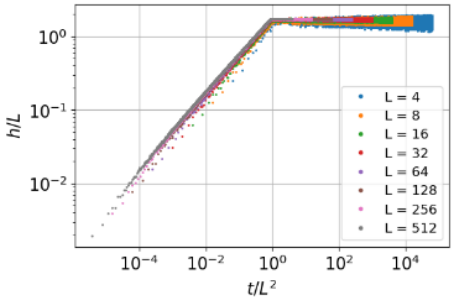

(a) The log-log plot of the data collapse on the pile height distribution.

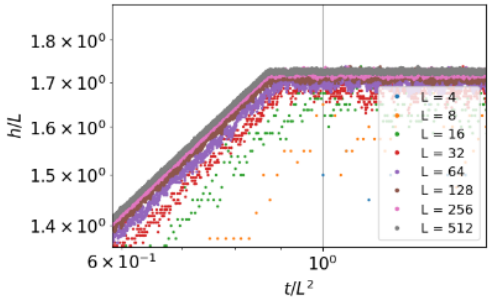

(b) The data collapse zoomed into the area where the sharp cutoff occurred. The larger the L, the sharper the cutoff is. The cutoff does not occur exactly at $t/L^2 = 1$ due to the presence of a constant of proportionality which is not 1. The recurrent state levels off at around $h/L \approx 1.73$ which agrees with the constant of proportionality found in task 2e.

Figure 5: The data collapse on the height of the pile.

2.5 Task 2e

For the remaining parts of task 2, only the heights of the pile for one realisation was considered, hence the seed number used was 1. In that realisation, only the heights for times $t \geq t_0$ where $t_0 > t_c$ were considered. t_0 was simply chosen as $t_0 = t_c + 100$. For the system sizes mentioned in task 2a, the average height $\langle h(t; L) \rangle$, the standard deviation of the height $\sigma_h(L)$ and the height probability $P(h; L)$ were measured.

Figure 6(a) shows the plot of the average height as a function of the system size L. Initially, the points indicate the relationship between $\langle h(t;L)\rangle$ and L is linear but we are interested if it contains signs of corrections to scaling. Hence, a scaling form was incorporated into the function such that

$$\langle h(t;L)\rangle = a_0 L(1 - a_1 L^{-w_1}) \tag{2}$$

obtained from [1]. This equation was made into a function which takes L, a_0, a_1 and w_1 as inputs. The data points were fitted with the function above using curve-fit method from scipy. This method also gives the error from the respective co-variance matrix. Table 1 shows the results for the values of the constants in eq. 2. To see the corrections to scaling more clearly, a plot of $\langle h\rangle/a_0 L$ against L was produced and shown in figure 6(b). It indicates eq. 2 does indeed capture the behaviour of average height for small L to a good degree. For large L, the plot tends to 1 verifying that the average height scales linearly with L for $L \gg 1$. Therefore, we can conclude the corrections to scaling is important for small L.

Constant	Value
a_0	1.7341 ± 0.0006
a_1	0.232 ± 0.013
w_1	0.609 ± 0.018

Table 1: The result from the curve-fit method. The errors in these values are small suggesting eq. 2 fits the points well.

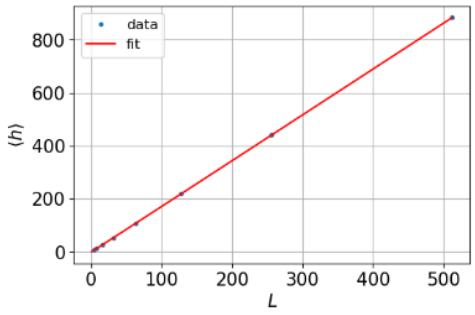

(a) The plot of $\langle h\rangle$ against L. The fit(red) line was plotted using the values obtained in table 1.

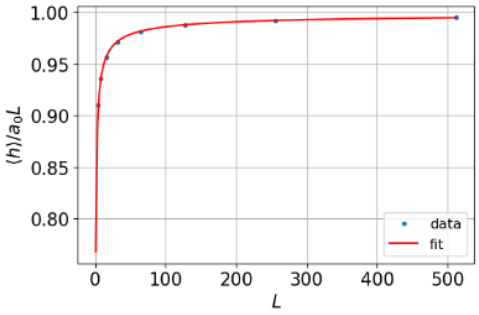

(b) The plot of $\langle h\rangle/a_0 L$ against L using the values obtained in table 1. For small L, the data deviates to a high degree from the value of 1 indicating it is limited by the system size L.

Figure 6: The plots to investigate the scaling of $\langle h\rangle$ with respect to L.

2.6 Task 2f

The log-log plot of standard deviation of height σ_h as a function of L is shown in figure 7(a). The straight line with a positive gradient clearly shows σ_h obeys a power law. These points were fitted with a power law equation of $\sigma_h = AL^{\alpha}$. Table II shows the result obtained for the values of the constants A and α. Figure 7(b) shows there is no corrections to scaling in the standard deviation of height, unlike $\langle h(t;L)\rangle$.

Constant	Value
A	0.583 ± 0.003
α	0.240 ± 0.001

Table 2: The result from the curve-fit method.

Let us now consider the average slope of the pile $\langle z_L\rangle$ which is defined as $\langle z_L\rangle = \langle h\rangle/L$. From task 2e, we know $\langle h\rangle = a_0 L$ in the limit of $L \to \infty$. Substituting this into the definition of $\langle z_L\rangle$, we get $\langle z_L\rangle$ approaching a_0 in the limit of $L \to \infty$. By definition, the standard deviation in $\langle z_L\rangle$, σ_z is σ_h/L. We know previously $\sigma_h = AL^{\alpha}$, hence $\sigma_z = AL^{\alpha-1}$. Since $\alpha - 1$ is less than 1, σ_z tends to zero in the limit of $L \to \infty$.

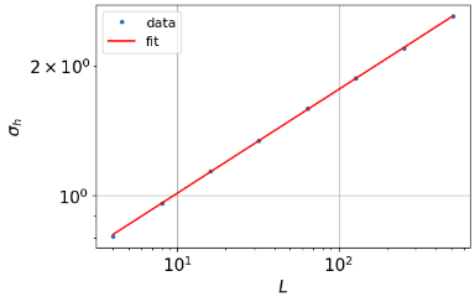

(a) The log-log plot of σ_h as a function of L. The red line represents $\sigma_h = 0.583L^{0.24}$.

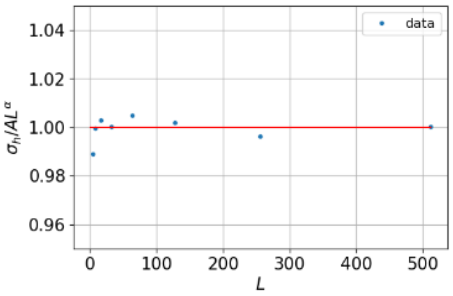

(b) The plot of σ_h/AL^{α} against L. There is no clear pattern in the plot suggesting there is no correction to scaling. Instead all values are close to 1 (red horizontal line) as expected.

Figure 7: The plots to investigate the scaling of σ_h with respect to L.

2.7 Task 2g

It is assumed that z_i in eq. 1 are independent, identically distributed random variables with finite variance. Hence, using eq. 1, $P(h;L)$ is expected to have a normal distribution by Central Limit Theorem (CLT) when $L \gg 1$ [3]. A plot of $P(h;L)$ against h was produced for various L and is shown in figure 8. For large enough L, the plot has the form of a normal distribution, agreeing with the theorem above. This peaks on each distribution also agree with the corresponding value of average height found in task 2e. We could

use the values of $\langle h \rangle$ and σ_h measured previously to perform a data collapse. In order to obtain a data collapse, the distributions must be standardized so the mean of the standard distribution will be zero with the standard deviation of 1 [3]. Every normal distribution is a version of the standard normal distribution whose domain has been stretched by the standard deviation and then translated by the mean value. Mathematically, in this case, one can write

$$P(h; L) = \frac{1}{\sigma_h} \varphi \left(\frac{h - \langle h \rangle}{\sigma_h} \right) \tag{3}$$

where φ is the standard distribution described above [3]. The factor $1/\sigma_h$ ensures $P(h; L)$ is normalised. Hence, I plotted $\sigma_h P(h; L)$ against $\frac{h - \langle h \rangle}{\sigma_h}$ so the left-hand side of eq. 3 has only one variable. The resulting plot is shown in figure 9. It is clear that the plot traces out a normal distribution with a mean of zero and a standard deviation of 1. From the assumptions made for the local slopes z_i, one can infer z_i is distributed normally with mean μ_z and standard deviation σ_z. From CLT, we know the average slope, $z_n = \frac{1}{L} \sum_{i=1}^{L} z_i$ has a normal distribution of $N(\mu_z, {\sigma_z}^2/L)$ obtained from [3]. Using eq. 1, we can find h has a normal distribution of $N(L\mu_z, L{\sigma_z}^2)$, giving $\sigma_h \propto \sqrt{L}$. However, from task 2f, we know $\sigma_h \propto L^{0.24}$. This deviation from the measured value suggests that the assumptions made were not entirely valid and the local slopes are indeed not independent. This is supported by the fact that not all configurations of local slopes are possible in the system. This might explain the very slight shift of the normal distribution plot in figure 9 since the peak is not exactly at zero.

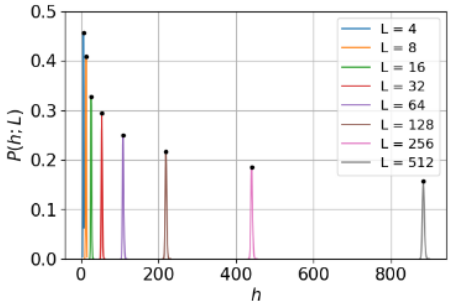

Figure 8: The plot of $P(h; L)$ against h. The black points indicate the average heights obtained from task 2e. Here, I interpolated the data points to highlight that they are following a Gaussian distribution.

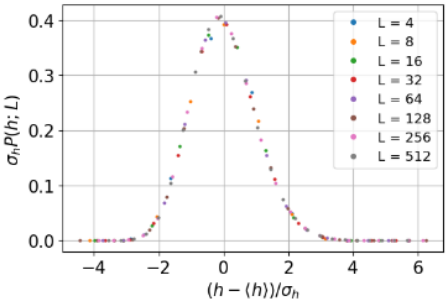

Figure 9: The plot of the data collapse on $P(h; L)$ which maps out the standard distribution function φ. However, there is a slight shift since the peak of the plot does not exactly lie on zero. This could either be due to a numerical error or the local slopes being not independent resulting in a skewed plot.

3 Task 3: The avalanche-size probability $P(s;L)$

The avalanche size s is defined as the number of relaxations caused by adding a grain at site $i = 1$. This includes zero avalanches ($s = 0$) too for normalisation. Only the avalanches after the system has reached steady state were considered, i.e. only for times $t \geq t_0$ as defined above.

3.1 Task 3a

The list of avalanche sizes s measured were $[s_{t_0}, s_{t_0+1}, ...]$ where s_{t_0} is the avalanche size at time t_0. A log-bin function for which the code was given, was used to analyse the list above. The function calculates log-bin frequency of unique integers in the list and returns the probabilities $P(s;L)$ for each bin. The other input of this function is the scale which controls the growth of bin sizes. The scale was chosen as 1.15 to allow reasonable growth. The 'zeros' input was always set as *True* to include $s = 0$ as mentioned. The number of samples N was chosen to be at least 770,000 to ensure the curve is relatively smooth, especially for large L. The plot of $P_N(s;L)$ versus s for different L is shown in figure 10. For all L, the straight line with a negative gradient indicates they obey a power law decay. This is followed by a bump which can be characterised by a cutoff avalanche size, s_c. The s_c appears to be increasing with the system size L. For $s > s_c$, the avalanche-size probability decays rapidly.

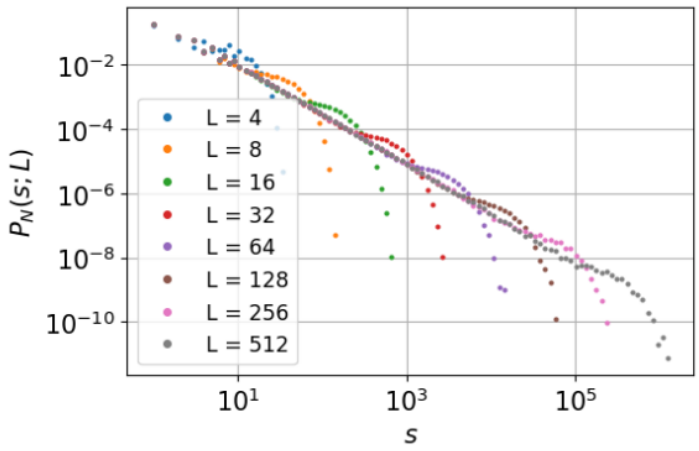

Figure 10: The log-log plot of avalanche-size probability $P_N(s;L)$ against the avalanche s for various L. The $s = 0$ was omitted in this plot.

3.2 Task 3b

It is suspected that $P_N(s;L)$ is consistent with the finite-size scaling ansatz

$$P_N(s;L) \propto s^{-\tau_s}\mathcal{G}\left(s/L^D\right) \tag{4}$$

for $L \gg 1$, $s \gg 1$ obtained from [1]. To test this, we could perform a data collapse. Firstly, to extract the critical exponent τ_s, the power law decay was investigated. Using the data for $L = 512$, the linear part of the log-log plot was fitted with a power law as shown in figure 11. The value of τ_s obtained was 1.551 ± 0.008. The first collapse was done vertically by plotting $s^{\tau_s}P_N(s;L)$ against s as shown in figure 12(a). The avalanche dimension D in eq. 4 was found by trial and error by plotting $s^{\tau_s}P_N(s;L)$ against s/L^D and observing if a reasonable data collapse has been achieved. The approximate value of D obtained was 2.25 and the resulting plot of data collapse is shown in figure 12(b).

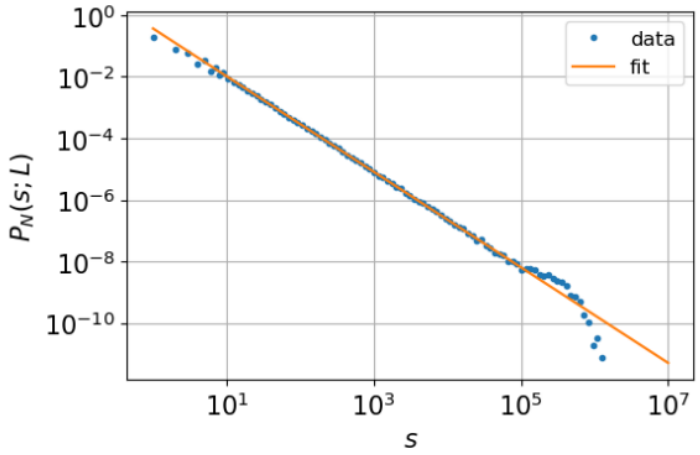

Figure 11: The log-log plot of avalanche-size probability $P_N(s;L)$ versus s for $L = 512$. Few of the first and final points were ignored to focus on the linear part which signifies power law decay. The orange fit line corresponds to the power law with exponent $\tau_s = 1.551$.

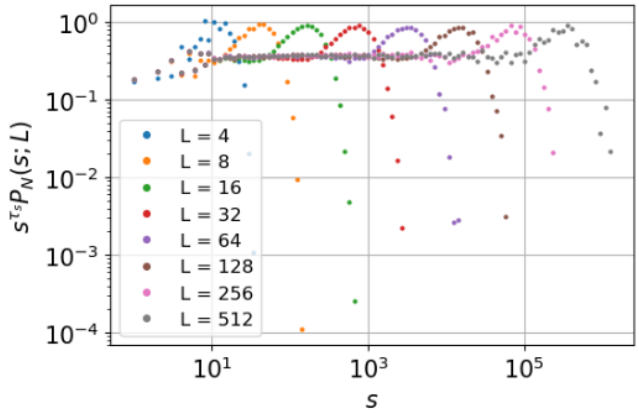

(a) The log-log plot of $s^{\tau_s}P_N(s;L)$ against s for $\tau_s = 1.551$.

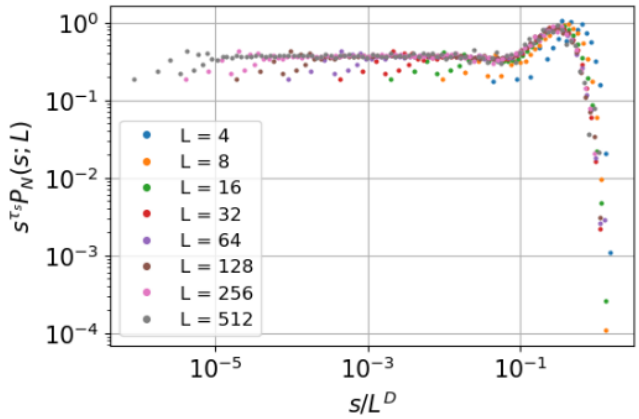

(b) The log-log plot of $s^{\tau_s}P_N(s;L)$ against s/L^D for $\tau_s = 1.551$ and $D \approx 2.25$. The data collapse is less reasonably satisfied for small L such as $L = 4$. This is because the scaling ansatz is only really valid for $L \gg 1$, $s \gg 1$. For $L > 8$, the plots agree with the data collapse to a reasonably well.

Figure 12: Data collapse on the avalanche size probability $P_N(s;L)$.

3.3 Task 3c

In addition to the data collapse, we could also find the estimates of critical exponents of τ_s and D by performing moment analysis on $P_N(s; L)$. The k'th moments of avalanche sizes $\langle s^k \rangle$ were measured for $k = 1, 2, 3, 4$. Assuming the finite-size scaling ansatz given in eq. 4 is true, we know that

$$\langle s^k \rangle \propto L^{D(1+k-\tau_s)} \tag{5}$$

for $L \gg 1$, $s \gg 1$, obtained from [2]. Figure 13 shows the plot of k'th moments against L seem to have a power law behaviour, suggesting eq. 5 could be valid. For each k, a power law was fitted for the last four points and the corresponding exponents were obtained with their errors. These exponents were plotted as a function of k as shown in figure 14. A linear function was fitted on these points, and the slope, m and the intercept, c were obtained along with their uncertainties. From the exponent in eq. 5, $D = m$ and $\tau_s = 1 - c/m$. The results obtained are shown on table 3 and they agree with the values found in task 3b. When $k = 1$, the average avalanche size should scale linearly with L and this is indeed what we find since $D(2 - \tau_s)$ is very close to 1.

Constant	Value
τ_s	1.5574 ± 0.0052
D	2.2417 ± 0.0042

Table 3: The result from the moment analysis of $P_N(s; L)$. The errors were obtained from the curve-fit method.

From figure 13, we could see the k'th moments do not agree well with the line of best fit for smaller L. This suggests there is a scaling effect. To investigate this further, I used a correction to scaling similar to eq. 2 for $k = 1$,

$$\langle s \rangle = b_0 L^{D(2-\tau_s)}(1 - b_1 L^{-y_1}). \tag{6}$$

This new function was fitted to the numerical data and the values of the constants were obtained as shown on table 4. Figure 15 shows the data for small L displays strong deviation from the value 1. Hence, we can conclude the corrections to scaling in the k'th moment of s is important for small L.

Constant	Value
b_0	1.14 ± 0.03
b_1	0.13 ± 0.02
y_1	0.08 ± 0.02

Table 4: The result from the curve-fit method. The errors are relatively high for y_1 suggesting we might need higher order terms in the scaling function.

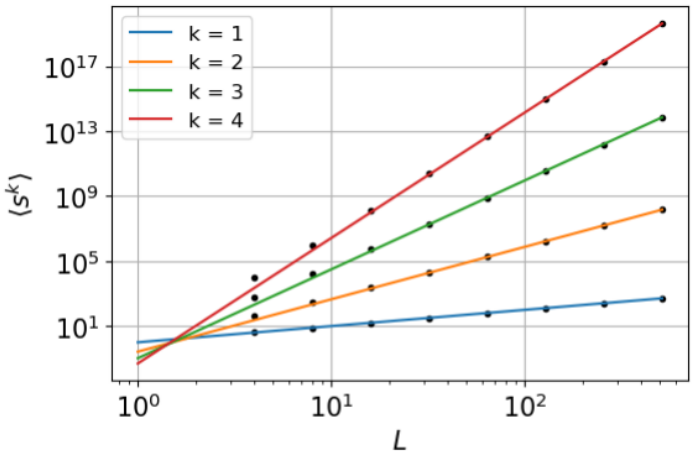

Figure 13: The log-log plot of $\langle s^k \rangle$ against L. Only the last four points were used for the fit to follow the condition for the ansatz that $L \gg 1$, $s \gg 1$. Data for small L do not agree well with the fit lines.

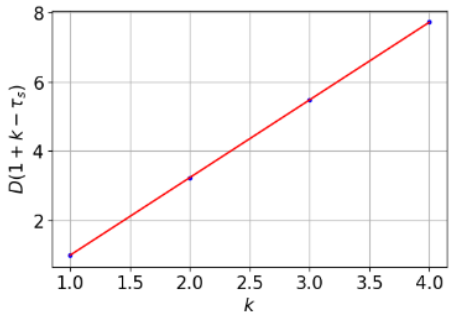

Figure 14: The plot of estimated exponent $D(1+k-\tau_s)$ versus k. The errorbars included are too small to be visible.

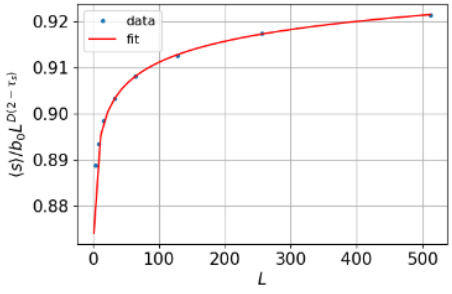

Figure 15: The plot $\langle s \rangle / b_0 L^{D(1+k-\tau_s)}$ versus L. The red curve is the fit found using the values on table 4. Smaller L deviate from the value 1 to a high degree. The correction needed in the case of $L = 4$ is approximately 11%.

References

[1] K.Christensen, *Complexity Project Notes*, Imperial College London, 6th January 2020.

[2] K.Christensen and N.Maloney, *Complexity and Criticality*, Imperial College Press, London, 2005.

[3] Daly, F., and Open University. Elements of Statistics. Wokingham: Open U, Addison-Wesley, 1995. Print.